Effect on THz Surface Plasmons of A Density Modulated Relativistic Electron Beam in A Parallel Plane Semiconducting Structure

Research Article

Pratibha Malik*, Suresh C. Sharma and Rinku Sharma

Department of Applied Physics, Delhi Technological University, Delhi, India
*Corresponding author: pratibhamalik27@gmail.com

Abstract. The excitation of terahertz (THz) surface plasmons by a density modulated relativistic electron beam propagating in a parallel plane semiconducting structure is investigated. The interaction of the electromagnetic surface wave with density modulated electron beam in the guiding structure is examined in the present work, which shows a significant enhancement in the radiation wave. The growth rate of the instability increases linearly with modulation index and reaches the largest value when the phase matching condition is satisfied in the generation of THz radiation wave, i.e., when the phase velocity of the THz radiation wave is comparable to the velocity of modulated beam. In addition, the growth rate of instability scales as one-third power of beam current and modulation index. Moreover,the surface plasmons resonance can be tuned in THz frequency range by the conventional doping concentration of the semiconductors.

Keywords. THz surface plasmons; Semiconductors; Pre-bunching; REB

PACS. 73.20.mf

Received: March 13, 2015   **Accepted:** November 4, 2015

1. Introduction

In recent years, Electromagnetic THz radiation has received a great attention due to wide range of applications including remote sensing, high resolution imaging and analysis,

security applications such as explosive detection, outer space communications and molecular spectroscopy [1–4]. The development of a compact high power and high efficient solid state devices for THz radiation has become a great challenge. Simultaneously, the growing interest in the field of surface plasmonics is converging in terahertz regime [5–7]. Surface plasmons are the electromagnetic waves which are bound to the surface of a conductor [8].

Narrow-band THz radiation can be produced by free-electron lasers [9] and fast diodes [10, 11]. Broadband THz radiation can also be produced by thermal sources. More recently, table-top laser-driven sources [12, 13] and short electron bunches in accelerators [14] with low power have been used to generate THz radiation. Antonsen and Palastro [15] have explained the excitation of the terahertz radiation by laser pulses in non uniform plasma channels. In this case, the propagation of the wave was considered in corrugated plasma channels. The corrugated channels and laser pulses with parameters were used to find energy conversion efficiency rate of the fraction of a joule per centimetre.

However, Hamster *et al*. [16] have demonstrated the THz radiation generation by laser pulses propagating in plasmas. The low frequency force exerted by laser pulse on plasma electrons leads to a current which has a spectral width and measured by temporal duration of laser pulse. Leemans *et al*. [17] have measured the radiation in 0.3-19 THz spectral range and at 94 GHz, generated at the plasma-vacuum interface, which depends quadratically on the bunch charge from laser accelerated electron bunches.

Yugami *et al*. [18] have demonstrated experimentally the Cerenkov waked millimetre wave generation by using an ultrashort and ultrahigh laser power pulse in magnetized plasma. However, the generation of terahertz radiation by Cerenkov wakes, excited by a short laser pulse has been examined by Yoshii *et al*. [19]. Shen *et al*. [20] have reported tunable, few-cycle and multicycle coherent terahertz pulses generation from a temporally modulated relativistic electron beam. In this case, THz radiation frequency can be tuned from 0.26 to 2.6 THz with the band-width of 0.16 THz.

The surface plasmons of millimeter wavelength are much higher in metal for a gap of THz radiation due to high density of the carriers. On the other hand, the doped semiconductors have become good candidate for tuned terahertz frequency range. In particular, narrow-band gap semiconductors such as n-type GaAs and n-type InSb are the materials which are used to produce high confined surface plasmons of THz frequency range due to loss-less scattering at room temperature. In fact, the dielectric function of such kind of materials are remarkably similar to that of plasmons, which are supporting metals such as gold and silver in UV or visible frequency range [21, 22].

The coherent synchrotron radiation has been observed experimentally in storage ring, when a short laser pulse interacts with a small part of electron bunch [23, 24]. Neumann *et al*. [25] have observed that the modulated electron beams are important due to the generation of coherent radiation but modulation can cause unwanted instability in devices. Specifically, in a free electron laser, the proper pre-bunching at the desired emission frequency can enhance performance of the system. Recently, the study of free electron laser (FEL) [26–28] and Cerenkov free electron laser (CFEL) [29], which are the tunable sources of high power coherent radiation,

have a great deal of interest.

In the previous work, it has been studied about the excitation of surface plasmons in a parallel plane semiconducting (n-InSb) system by pre-bunched electron beam [31]. In this paper, we investigate the effect of a density modulated relativistic electron beam on the excitation THz surface plasmons. This scheme involves the amplification of the surface wave in the guiding system. The paper is organised in the following manner. In Section 2, a theoretical model of parallel plane guiding structure, is developed, which is made up of two parallel semiconducting slabs, separated by free-space. In Section 3, we present the analysis of the interaction of density modulated electron beam with surface plasmons in the waveguide, which gives the dispersion relation of the wave. An analytical expression for the transcendental wave equations is being expressed in Section 4. The results are discussed in Section 5.

2. Model

In this section, we investigate the excitation of THz surface plasmons by a density modulated relativistic electron beam, propagating in a parallel plane n-type GaAs semiconducting structure. The sketch of the structure is shown in Figure 1, which consists of two semi-infinite parallel plane semiconductor slabs separated with free-space. The electric field of the surface wave is assumed to have space and time dependence as $\exp(-i\omega t + ik_z z)$, propagating on the surface of the interfaces along z-direction. The propagation of the wave is not along y-direction i.e., $k_y = 0$ and $\frac{\partial y}{\partial x} = 0$. The Drude model for metal-semiconductor gives the relation for dielectric permittivity $\varepsilon_m(\omega)$, plasma frequency ω_p, radiation frequency ω, and electron phonon collision frequency ν [30].

$$\varepsilon_m(\omega) = \varepsilon_{latt} - \frac{{\omega_p}^2}{\omega^2(1 + i\nu/\omega)} \quad \text{or} \quad \varepsilon_m(\omega) = \varepsilon_{latt} + i\left(\frac{4\pi\sigma}{\omega}\right), \tag{1}$$

where σ is the conductivity of the semiconductor and ε_{latt} is the lattice permittivity. We consider the collisionless plasma and neglecting the electron phonon collision frequency of the medium, i.e., $\nu = 0$. The conductivity of the semiconductor is given by the relation

$$\sigma = \frac{n_s e^2}{m_e{}^*(\nu - i\omega)},$$

where ω_p $\left(= \sqrt{\frac{4\pi e^2 n_s}{m_e^*}}\right)$ is the plasma frequency, $-e$, m_e^* and n_s are the electronic charge, effective mass and density of plasma electrons in the semiconductor, respectively. Furthermore, the electromagnetic field equations in each layer of the parallel plane waveguide, are described as

$$\frac{\partial^2 \vec{E}}{\partial x^2} + (k_z{}^2 \varepsilon_m(\omega) - \beta^2)\vec{E} = 0, \tag{2}$$

where $k_x^2 = \beta^2 - \frac{\omega^2 \varepsilon_m(\omega)}{c^2}$ and $\beta = \left(k_z{}^2 - \frac{\omega^2 \varepsilon_m(\omega)}{c^2}\right)^{\frac{1}{2}}$

$$\beta = \begin{cases} \beta_1 \\ \beta_2 \end{cases} \quad \text{when} \quad \begin{array}{l} \varepsilon_m(\omega) = \varepsilon_{sc} \quad \text{for } x < -r \text{ and } x > +r, \\ \varepsilon_m(\omega) = 1 \quad \text{for } -r < x < +r. \end{array}$$

The total electric field E in x- and z-directions

$$\vec{E} = \begin{cases} c_1\left(\frac{-ik_z\hat{x}}{\beta_1} + \hat{z}\right)e^{\beta_1 x}e^{-i(\omega t - k_z z)} & \text{for } x < -r, \\ c_3\left(\frac{ik_z\hat{x}}{\beta_1} + \hat{z}\right)e^{-\beta_1 x}e^{-i(\omega t - k_z z)} & \text{for } x > r, \\ \left(c_2\left(\frac{-ik_z\hat{x}}{\beta_2} + \hat{z}\right)e^{\beta_2 x} + c_2'\left(\frac{ik_z\hat{x}}{\beta_2} + \hat{z}\right)e^{-\beta_2 x}\right)e^{-i(\omega t - k_z z)} & \text{for } -r < x < r. \end{cases} \tag{3}$$

This has been chosen for SPW that $\nabla \cdot \vec{E} = 0$, and for two surfaces $\varepsilon_m(\omega)E_x$, E_z are continues at $x = -r$ and at $x = +r$, therefore, on applying the boundary conditions with equation of continuity, i.e., we get the relations: $c_1 = c_3$ and $c_2 = c_2'$ (symmetric mode).
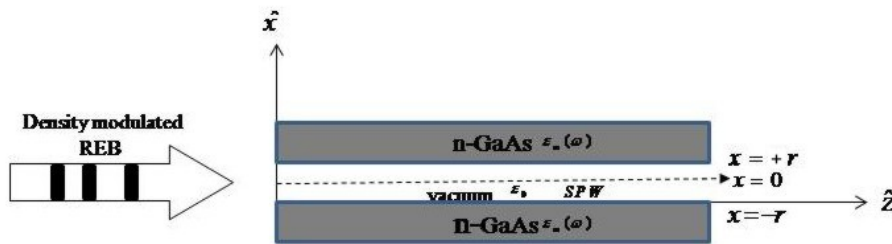

Figure 1. Sketch of a modulated beam on the excitation of THz radiation in a parallel plane semiconducting structure.

3. Dispersion Relation for Surface Plasmons

In order to calculate the relation between the wave vector k_z and electromagnetic wave frequency ω in the waveguide, we use the dispersion relation of the surface plasma wave and we get the relation as

$$c_1 = 2c_2\cosh(r\beta_2)e^{r\beta_1} \quad \text{and} \quad \varepsilon_m(\omega)\tanh(r\beta_2) = -\frac{\beta_2}{\beta_1}$$

using the above equations, the dispersion relation formed as

$$k_z = \left[\frac{\varepsilon_m(\omega)\omega^2(\varepsilon_m(\omega) - \tanh^2(r\beta_2))}{c^2(\varepsilon_m{}^2(\omega) - \tanh^2(r\beta_2))}\right]^{\frac{1}{2}}. \tag{4}$$

Case 1: If $r\beta_2 \gg 1$, Eq. (4) turns out to be as $k_z^2 = \frac{\omega^2\varepsilon_m(\omega)}{c^2(\varepsilon_m(\omega)+1)}$, which is the conventional surface plasma wave dispersion relation on a single interface. Since surface plasmons are bound to the surface of the interface so these remain localized near the semiconductor-vacuum interface.

Case 2: While, the term $\tanh(r\beta_2)$ can not be neglected in Eq. (4), as $r\beta_2 > 1$, in the guiding structure and solving it iteratively. One may obtain the dispersion relation as

$$k_z = \left[\frac{\omega^2\varepsilon_m(\omega)}{c^2(\varepsilon_m(\omega)+1)}\left(1 + \frac{4\varepsilon_m(\omega)e^{-2r\beta_2}}{\varepsilon_m^2(\omega) - 1}\right)\right]^{\frac{1}{2}}. \tag{5}$$

Figure 2 is a plot of k_z versus ω by using Eq. (5), which shows that the frequency of the radiation wave increases with axial wave vector i.e., the speed of light linearly dependent on the wavelength.

4. Amplification of Surface Plasmons by A Density Modulated Relativistic Electron Beam

Consider a modulated relativistic electron beam of density $n = n_{0b} + n_{so} \exp[-i(\omega_0 t - k_{z0} z)]$, propagating in the centre of parallel plane guiding structure with velocity $v_{ob} \left(\approx \frac{\omega_0}{k_{z0}}\right)$, (where $\Delta \left(= \frac{n_{so}}{n_{ob}}\right)$ being the modulation index, which ranges from 0 to 1, ω_o is the modulation frequency and k_{z0} is the modulated wave vector of the beam). The Gaussian density profile of the beam represented by relation $n_{ob} = N_{0b} e^{-x^2/a_b^2}$, where N_{ob} is the beam electron density with radius a_b. While the beam current is expressed as $I_b = \sqrt{\pi} N_{0b} e a_b w_b v_{ob}$, where w_b is width of the beam. The response of plasma electrons in the medium is governed by equation of motion. On solving these equations, we obtain the perturbed velocity components along x-and z-directions as

$$v_{bx} = \frac{e}{im\omega\gamma_0}\left(E_x + \frac{v_{ob}}{i(\omega - k_z v_{ob})}\frac{\partial E_z}{\partial x}\right), \tag{6}$$

$$v_{bz} = \frac{eE_z}{im(\omega - k_z v_{ob})(\gamma_0^3)}. \tag{7}$$

The relativistic gamma factor is $\gamma_0 = \left(1 - \frac{v_{ob}^2}{c^2}\right)^{-\frac{1}{2}}$. From Equation of Continuity, we have

$$\frac{\partial n}{\partial t} + \nabla \cdot (n\vec{v}) = 0,$$

where

$$\vec{v} = v_{0b}\hat{z} + \vec{v}_b \exp[-i(\omega t - k_z z)]$$

and

$$n = n_{ob} + \Delta n_{ob} \exp[-i\omega_o(t - z/v_{ob})] + n_{1b}\exp[-i(\omega t - k_z z)],$$

with $\vec{v}_b = v_{bx}\hat{x} + v_{bz}\hat{z}$. We obtain the perturbed beam density as

$$n_{1b} = \frac{\left[(1+\Delta)v_{bx}\frac{\partial n_{ob}}{\partial x} + (1+\Delta)n_{ob}(\nabla \cdot \vec{v}_b)\right]}{i(\omega - k_z v_{ob})}. \tag{8}$$

The perturbed current density becomes

$$\vec{J}^{nl} = -en_{ob}\vec{v}_b - \Delta en_{ob}\vec{v}_b - en_{1b}v_{ob}\hat{z}. \tag{9}$$

To study the instability of the unstable mode retaining only those terms which go as $(\omega - k_z v_{ob})^{-2}$, and discarding the first and second term of Eq. (9). We obtain the perturbed current density as

$$\vec{J}^{nl} = -\frac{e^2 v_{ob}(1+\Delta)}{im}\left[-\frac{v_{ob}}{\omega\gamma_0(\omega-k_z v_{ob})^2}\frac{\partial n_{ob}}{\partial x}\frac{\partial E_z}{\partial x} - \frac{n_{0b}v_{ob}}{\omega\gamma_0(\omega-k_z v_{ob})^2}\frac{\partial^2 E_z}{\partial x^2}\right.$$
$$\left. + \frac{n_{ob}}{\gamma_0^3(\omega-k_z v_{ob})^2}\frac{\partial E_z}{\partial z}\right]\hat{z}. \tag{10}$$

Now, replacing $k_z = \frac{\omega}{v_{ob}}$ and $\frac{\partial^2}{\partial x^2} = \beta_2^2$, in Eq. (10), the perturbed current density can be re-written as

$$\vec{J}^{nl} = \frac{e^2(1+\Delta)v_{ob}^2}{im\omega\gamma_0(\omega - k_z v_{ob})^2} \frac{\partial n_{ob}}{\partial x} \frac{\partial E_z}{\partial x} \hat{z}. \tag{11}$$

The electric and magnetic field of surface plasmons are related with the equations $\vec{E} = A_1(t)\vec{E}_o$ and $\vec{H} = A_2(t)\vec{H}_0$, when the beam current is present, where $\vec{E}_o$ and $\vec{H}_0$ are the electric and magnetic field in the absence of beam current. In vacuum region permittivity is $\varepsilon_m = 1$. The relations are defined as $\nabla \times \vec{E}_0 = \frac{i\omega}{c}\vec{H}_0$ and $\nabla \times \vec{H}_0 = -\frac{i\omega\varepsilon_m}{c}\vec{E}_0$, where

$$\nabla \times \vec{E} = -\frac{1}{c}\frac{\partial\vec{H}}{\partial t} \quad \text{and} \quad \nabla \times \vec{H} = \frac{4\pi}{c}(\vec{J}^{nl} + \vec{J}_s^{nl}) + \frac{\varepsilon_{latt}}{c}\frac{\partial\vec{E}}{\partial t} \tag{12}$$

using Eq. (12), one may find the equations as $\frac{\partial A_2}{\partial t} \approx \frac{\partial A_1}{\partial t}$ and $\frac{\partial A_2}{\partial t} = i\omega(A_1 - A_2)$ with

$$\left[\frac{\partial A_1}{\partial t} - i\omega(A_1 - A_2)\right]\vec{E}_0 = -4\pi\vec{J}^{nl}. \tag{13}$$

Multiplying Eq. (13) by $E_0{}^*$ and integrating from $-\infty$ to $+\infty$, we obtain

$$\left[\frac{\partial A_1}{\partial t} + FA_1\right] = -\frac{2\pi\int_{-\infty}^{+\infty}\vec{J}^{nl}\cdot\vec{E}_0^* dx}{\int_{-\infty}^{+\infty}\vec{E}_0\cdot\vec{E}_0^* dx} = \frac{4(1+\Delta)\omega_{pb}^2 v_{0b}^2\beta_2 M}{\gamma_0\omega(\omega-k_z v_{ob})^2 a_b^2 N}A_1 \tag{14}$$

where

$$N = \frac{[1+\cosh(2\beta_2 r)](\beta_1^2 + k_z^2)}{\beta_1^3} + \frac{2[(2\beta_2 r(\beta_2^2 - k_z^2) + (\beta_2^2 + k_z^2)\sinh(2\beta_2 r)]}{\beta_2^3},$$

$$M = \int_{-r}^{+r}\cosh(\beta_2 x)\sinh(\beta_2 x)\exp\left(\frac{-x^2}{a_b^2}\right)x\,dx.$$

Therefore, the relation becomes

$$\frac{\partial A_1}{\partial t} + FA_1 = \frac{4(1+\Delta)\omega_{pb}^2 v_{ob}^2\beta_2 M}{\omega\gamma_0 a_{0b}^2 N}A_1. \tag{15}$$

Where $F = ik_z v_{gr}$, and $\omega_{pb}(=(4\pi N_{ob}e^2/m)^{1/2})$ is the beam plasma frequency, $\frac{\partial}{\partial t} = -i\delta$, δ is the frequency mismatch and v_{gr} is the group velocity of the radiation frequency ω, respectively. We write $\omega = k_z + i\delta$ and the imaginary part gives the growth rate

$$\Gamma = \text{Im}\,\delta = \left(\frac{4(1+\Delta)\omega_{pb}^2 v_{ob}^2\beta_2 M}{\omega\gamma_0 a_b^2 N}\right)^{\frac{1}{3}}e^{i(2n\pi/3)}, \quad n = 0, 1, 2. \tag{16}$$

Eq. (16) can be re-written as

$$\Gamma = \frac{\sqrt{3}}{2}\left(\frac{4(1+\Delta)\omega_{pb}^2 v_{ob}^2\beta_2 M}{\omega\gamma_0 a_b^2 N}\right)^{\frac{1}{3}}. \tag{17}$$

From Eq. (17), we can say that the growth rate Γ of the THz radiation mode scales as the one-third power of the beam current and modulation index Δ.

5. Results and Discussion

The numerical calculations have been carried out using the typical parameters for SPs (a) For n-type GaAs semiconductor: electron plasma density $n_s = 0.9 \times 10^{17}$ cm^{-3}, the effective mass of the semiconductor $m^* = 0.067m$ and lattice permittivity ε_{latt} is 10.89, (b) For n-type InSb: the electron plasma density $n_s = 2 \times 10^{16}$ cm^{-3}, the effective mass of the semiconductor $m^* = 0.014m$, lattice permittivity ε_{latt} is 15.7, and other parameters are same and kept constant as given: mass of electron $m = 9.1 \times 10^{-28}$ g, charge of electron $e = 4.8 \times 10^{-10}$ statcoulombs, and modulation index Δ ranges from 0 to 1 in the steps of 0.1. The parallel semiconducting plate separated with a distance of $2r = 0.72$ cm. However, the electron beam width and radius are defined as 0.60cm $\hat{y}$ and 0.32 cm, respectively.

Using Eq. (5), we have plotted the dispersion curve of surface plasma wave (cf. Figure 2). From Figure 2, it can be seen that the radiation frequency ω increases with the propagation vector k_z of the unstable mode. Figure 3, shows the graph between the plasma frequency and density of plasma electrons of the semiconductor. It can be seen form Figure 3, that the plasma frequency increases with density of electrons, which follows the same trend of results obtained by Kong *et al.* [32]. In Figure 4, we have plotted the growth rate Γ (rad/sec) of the unstable mode as a function of modulation index Δ using Eq. (17) for the following parameters: $\omega/\omega_p = 0.47$, $E_b = 2.7$ MeV, $\omega_p/\omega_{pb} = 5.31 \times 10^3$, normalized distance $r\omega_p/c = 783.9$. From Figure 4, it can be observed that the growth rate of the instability increases linearly with the modulation index and reaches the largest value when $\Delta \sim 1$, $k_z \sim k_{zo}$ and $\omega \sim \omega_o$, which satisfied the condition of phase matching in the generation of THz wave i.e., when the phase velocity of the THz radiation wave is comparable to the modulated beam velocity.
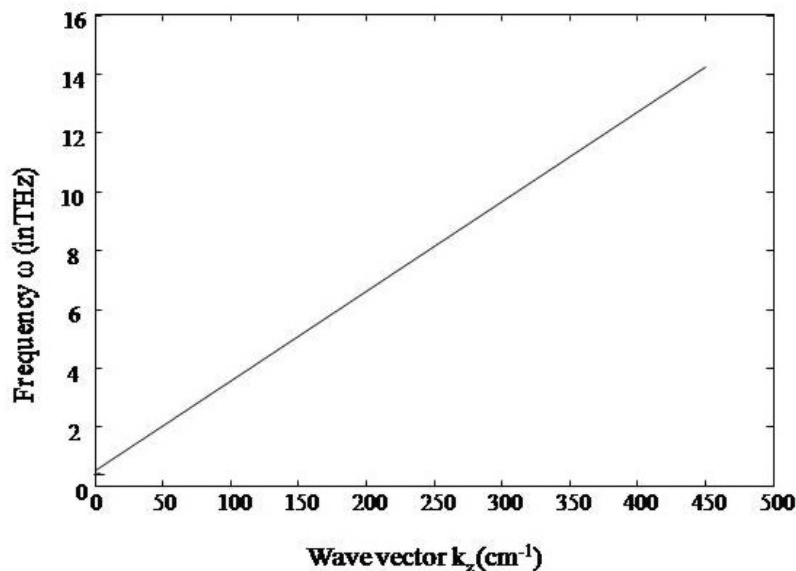

Figure 2. Dispersion curve of SPW for n-type GaAs semiconductor:radiation frequency ω is a function of axial wave vector k_z at the values $2r = 0.72$ mm and $\varepsilon_{latt} = 10.89$.
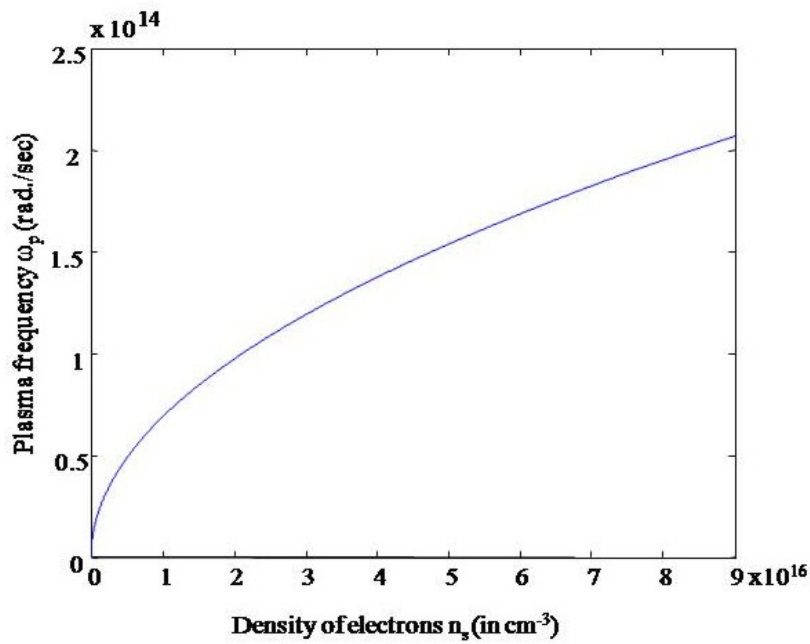
Figure 3. Plot of plasma frequency ω_p (in rad./sec) versus plasma density of electrons n_s (in cm^{-3}) for n-type GaAs.
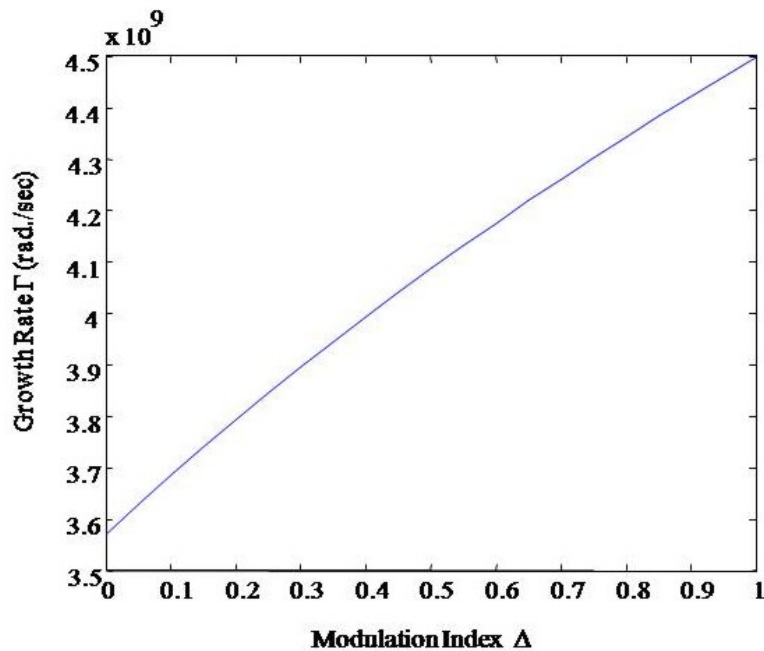

Figure 4. Plot of growth rate Γ (in rad./sec) of instability versus modulation index Δ at $\omega/\omega_p = 0.47$ and $E_b = 2.7$ MeV.

From Eq. (17) it can be seen that the growth rate of the unstable mode scales as the one-third power of the beam density. The modulated beam electrons transfer their energy to the electromagnetic surface plasmons, till the velocity of beam electrons is slightly greater than

the phase velocity of the THz wave, which leads a significant amplification in the amplitude of the unstable wave. In Figure 5, we plotted a graph between the growth rate of instability and modulation index for n-type GaAs and n-type InSb for the same parameters as mentioned above. From Figure 5, it can be seen that the growth rate of n-type InSb, a narrow band gap semiconductor, is higher than the n-type GaAs semiconductor.
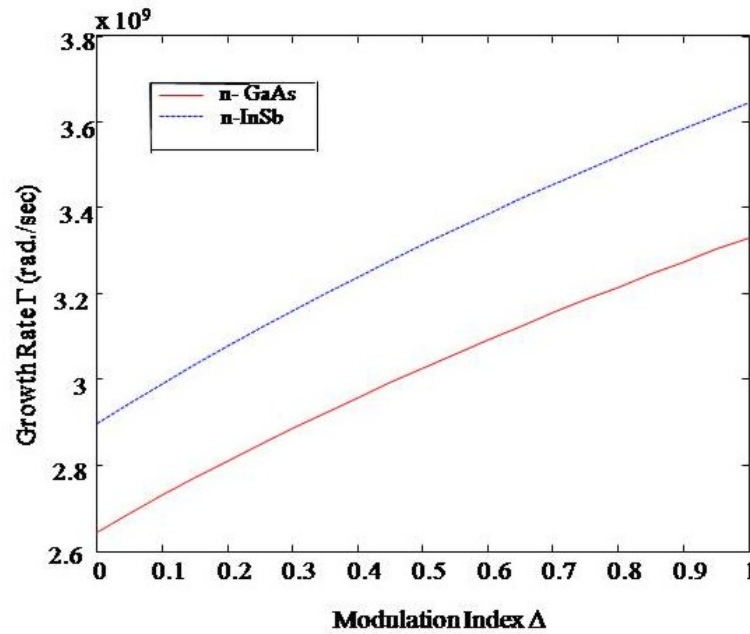

Figure 5. Variation of growth rate Γ (in rad./sec) of the instability with modulation index Δ for the semiconductors (a) n-type InSb (dash) (b) n-type GaAs ((solid).

6. Conclusion

A theoretical model for the interaction of density modulated electron beam with thermally emitted surface plasmons in a parallel plane guiding structure (n-type GaAs), is studied in the present paper. The growth rate of unstable mode of THz surface plasmons gets amplified with modulation index and reaches the largest value as $\Delta \sim 1$, and satisfies the condition of phase matching i.e., when the velocity of modulated beam is comparable to the phase velocity of the radiation wave. In addition, the growth rate of instability scales as one third power of beam density. Furthermore, we compare the thermal emission property of the n-type GaAs and n-type InSb. In this case, it is found that the growth rate of instability mode for n-type InSb is higher than the n-type GaAs semiconductor. It is concluded that the main mechanism for the high growth rate in instability for n-type InSb sample may be due to high conductivity of the electrons. The analysis also illustrates that the surface plasmons resonance can be tuned within frequency range from 0.3 to 10 THz by conventional doping concentration of the semiconductors. In conclusion, n-type InSb semiconductor with a small band gap strongly supports the confinement of surface plasmons in a parallel plane guiding structure.

Competing Interests

The authors declare that they have no competing interests.

Authors' Contributions

All the authors contributed significantly in writing this article. The authors read and approved the final manuscript.

References

[1] M. Nagel, P.H. Bolivar, M. Brucherseifer, H. Kurz, A. Bosserhoff and R. Buttner, *Appl. Phys. Lett.* **80**, 154 (2002).

[2] W. Zhang, A.K. Azad and D. Grischkowsky, *Appl. Phys. Lett.* **82**, 2841 (2003).

[3] C.M. Rhoads, E.K. Damon and B.A. Munk, *Appl. Opt.* **21**, 2814 (1982).

[4] C. Winnewisser, F. Lewen, J. Weinzierl and H. Helm, *Appl. Opt.* **38**, 3961 (1999).

[5] P.L. Marston, *Nature* **391**, 841 (1998).

[6] Y.X. Zhang, Y. Zhou, L. Dong and S.G. Liu, *Appl. Phys. Lett.* **102**, 211104 (2013).

[7] T.H. Isaac, J.G. Rivas, J.R. Sambles, W.L. Barnes and E. Hendry, *Phys. Rev. B* **77**, 113411 (2008).

[8] S.L. Dexheimer (ed.), *Terahertz Spectroscopy, Principles and Applications*, CRC Press (2008).

[9] G. Ramian, *Nucl. Instrum. Methods Phys. Res. A* **31**, 225 (1992).

[10] D.W. Porterfield, T.W. Crowe, R.F. Bradley and N.R. Erickson, *IEEE Trans. Microwave Theory Techn. MTT* **47**, 419 (1999).

[11] P.H. Siegel, Terahertz technology, *IEEE Trans. Microwave Theory Techn., MTT* **50**, 910 (2002).

[12] D.H. Auston, K.P. Cheung, J.A. Valdmanis and D.A. Kleinman, *Phys. Rev. Lett.* **53**, 1555 (1984).

[13] A. Bonvalet, M. Joffre, J.L. Martin and Migus, *Appl. Phys. Lett.* **67**, 2907 (1995).

[14] T. Nakazato, M. Oyamada, N. Niimura, S. Urasawa, O. Konno, A. Kagaya, R. Kato, T. Kamiyama, Y. Torizuka, T. Nanba, Y. Kondo, Y. Shibata, K. Ishi, T. Ohsaka and M. Ikezawa, *Phys. Rev. Lett.* **63**, 1245 (1989).

[15] T.M. Antonsen, Jr. and J. Palastro, *Phys. Plasmas* **14**, 0333107 (2007).

[16] H. Hamster, A. Sullivan, S. Gordon, W. White and R. Falcone, *Phys. Rev. Lett.* **71**, 2725 (1993).

[17] W.P. Leemans, J. van Tilborg, J. Faure, C.G.R. Geddes, Cs. Toth, C.B. Schroeder, E. Esarey, G. Fubiani and G. Dugan, *Phys. Plasmas* **11**, 2899 (2004).

[18] N. Yugami, T. Higashiguchi, H. Gao, S. Sakai, K. Takahashi, H. Ito, Y. Nishida and T. Katsouleas, *Phys. Rev. Lett.* **89**, 65003 (2002).

[19] J. Yoshi, C.H. Lai, T. Katsouleas, C. Joshi and W.B. Mori, *Phys. Rev. Lett.* **79**, 4194 (1997).

[20] Y. Shen, X. Yang, G.L. Carr, Y. Hidaka, J.B. Murphy and X. Wang, *Phys. Rev. Lett.* **107**, 204801 (2011).

[21] T.H. Isaac, W.L. Barnes and E. Hendry, *App. Phys Lett.* **93**, 241115 (2008).

[22] T.H. Isaac, J.G. Rivas, J.R. Sambles, W.L. Barnes and E. Hendry, *Phys. Rev. B* **77**, 113411 (2008).

[23] J.M. Byrd, Z. Hao, M.C. Martin, D.S. Robin, F. Sannibale, R.W. Schoenlein, A.A. Zholents and M.S. Zolotorev, *Phys. Rev. Lett.* **96**, 164801 (2006).

[24] F. Sannibale, J.M. Byrd, Á. Loftsdóttir, M. Venturini, M.A. Bakr, J. Feikes, K. Holldack, P. Kuske, G. Wüstefeld, H.W. Hubers and R. Warnock, *Phys. Rev. Lett.* **93**, 094801 (2004).

[25] J.G. Neumann, R.B. Fiorito, P.G.O. Shea, H. Loos, B. Sheehy, Y. Shen and Z. Wu, *J. App. Phys.* **105**, 053304 (2009).

[26] M. Cohen, A. Kugel, D. Chairman, M. Arbel, H. Kleinman, D. Ben Haim, A. Eichenbaum, M. Draznin, Y. Pinhasi, I. Yakover and A. Gover, *Nucl. Instrum. Methods Phys. Res. A* **358**, 82 (1995).

[27] P. Freund, P.G. O'Shea and J. Neumann, *Nucl. Instrum. Methods Phys. Res. A* **507**, 400 (2003).

[28] S.C. Sharma, J. Sharma, A. Bhasin and R. Walia, *J. Plasma Phys.* **78**, 635 (2012).

[29] J.M. Ortega, Y. Lapierre, B. Girard, M. Billardon, P. Elleaume, C. Bazin, M. Bergher, M. Velghe and Y. Petroff, *IEEE J. Quantum Electron* **21**, 909 (1985).

[30] C.S. Liu and V.K. Tripathi, *Electromagnetic Theory for Telecommunication*, Cambridge University Press (2007).

[31] S.C. Sharma and P. Malik, *Phys. Plasmas* **22**, 043301 (2015).

[32] B.D. Kong, V.N. Sokolov, K.W. Kim and R.J. Trew, *IEEE J. Sensors* **10**, 443 (2002).